Environ Model Assess (2014) 19:271–282
DOI 10.1007/s10666-013-9397-8

Integrated Traffic and Emission Simulation: a Model Calibration Approach Using Aggregate Information

Xiaoliang Ma · Zhen Huang · Haris Koutsopoulos

Received: 16 May 2012 / Accepted: 19 December 2013 / Published online: 14 January 2014

Abstract Environmental impacts of road traffic have attracted increasing attention in project-level traffic planning and management. The conventional approach considers emission impact analysis as a separate process in addition to traffic modeling. This paper first introduces our research effort to integrate traffic, emission, and dispersion processes into a common distributed computational framework, which makes it efficient to quantify and analyze correlations among dynamic traffic conditions, emission impacts, and air quality consequences. A model calibration approach is particularly proposed when on-road or in-lab instantaneous emission measurements are not directly available. Microscopic traffic simulation is applied to generate dynamic vehicle states at the second-by-second level. Using aggregate emission estimation as standard reference, a numerical optimization scheme on the basis of a stochastic gradient approximation algorithm is applied to find optimal parameters for the dynamic emission model. The calibrated model has been validated on several road networks with traffic states generated by the same simulation model. The results show that with proper formulation of the optimization objective function, the estimated dynamic emission model can capture the trends of aggregate emission patterns of traffic fleets and predict local emission and air quality at higher temporal and spatial resolutions.

Keywords Vehicle emission · Traffic pollution · Integrated modeling · Emission models · Model calibration · SPSA · Traffic simulation

X. Ma (✉) · Z. Huang · H. Koutsopoulos
Traffic and Logistics, Department of Transportation Sciences, Royal Institute of Technology (KTH), Teknikringen 72, Stockholm 10044, Sweden
e-mail: liang@kth.se

1 Introduction

Despite growing efforts in reducing emission pollution, the deterioration of air quality has proved to be persistent worldwide. As a result of continual growth of traffic, road transport has become by far the dominant anthropogenic source of environmental pollution in urban areas. It has stimulated the requirements for coherent development of management strategies for both traffic and its environmental impacts at the local network level as well as urban and regional scales.

In order to manage the urban air pollution induced by traffic flow, it is essential to accurately estimate the time-resolved emission quantity in the city road network. To fulfill such an objective, the majority of the research effort is based on, instead of direct measurement, computational modeling of emissions using the input of traffic dynamics as well as individual vehicle information. Different emission models have been developed to compute fuel consumption and air pollutants including CO, HC, NOx, and particulate matters (PMs) as well as greenhouse gases, e.g., CO_2. Similar to transport models, an emission model can be either macroscopic, mesoscopic, or microscopic in nature according to its detailed characteristics. In this paper, we summarize the models simply in two main categories: aggregate and microscopic emission models.

1.1 Aggregate Emission Models

Aggregate emission models are normally applied to estimate traffic emission quantity at the network level by considering traffic flow properties such as vehicle fleet composition, average flow speed, and vehicle travel distance as inputs. There are several well-known aggregate models such as MOVES and MOBILE [1] developed by US EPA, as well

as the Computer Programme to Calculate Emissions from Road Transport (COPERT) [2], Handbook Emission Factors for Road Transport (HBEFA) [3], and Assessment and Reliability of Transport Emission Models and Inventory Systems (ARTEMIS) [4] developed by the European countries. The ARTEMIS model is an emission model recently developed in the European Union (EU) using a large amount of on-road and in-lab emission data measured in different countries. The model is considered applicable for estimation of not only macroscopic but also short-term dynamic emission index for various sizes of road networks. The essential calculation in ARTEMIS depends on an encoded database, which incorporates emission factors derived from real measurements. To make it compatible with the previous modeling approach such as the COPERT, alternative modules are also provided so that users can compute emission measures using aggregate traffic flow variables on predefined networks (e.g., average traffic speed). In ARTEMIS and other EU emission models, vehicle classification is based on the fuel type and the EU Emission Standard, shown in the left column of Table 1.

In Sweden, different studies were carried out to compare on-road emission factors against the modeling results of COPERT IV, HBEFA, and ARTEMIS. In [5], essential measurements were conducted by means of remote optical sensors at roadside, and comparisons were made for the gasoline passenger vehicles at three locations. Acceptable agreement was concluded between the roadside measurement and estimation of ARTEMIS, although significant discrepancies appear occasionally.

1.2 Microscopic Emission Models

As increased attention is paid to traffic impact management in local networks, microscopic emission models have become a research topic of great interest. Taking vehicle operating conditions as inputs including instantaneous speed, acceleration, engine states, and so on, the models aim at predicting microscale vehicular emission at a second-by-second resolution. The development of microscopic emission models requires collection of emission data from various types of vehicles. Different approaches have been adopted in the model development including the physical power-based models (e.g., the CMEM model [6]) and the regression-based approach (e.g., the VT-Micro model [7]).

Whereas the power-based models are based on complex physical principles, the VT-Micro statistical model [7] uses a third-order polynomial regression of instantaneous vehicle speed and acceleration. It was developed first by Virginia Tech. using the Portable Emission Measurement System (PEMS) data collected in the USA. The second column of Table 1 illustrates the vehicle categories adopted in the original model development. Mathematically, the model can be simply represented by the following:

$$E_e = \begin{cases} \exp\left(\sum_{i=0}^{3}\sum_{j=0}^{3}\left(L_{i,j}^{e}\cdot v^i\cdot a^j\right)\right) & a \geq 0 \\ \exp\left(\sum_{i=0}^{3}\sum_{j=0}^{3}\left(M_{i,j}^{e}\cdot v^i\cdot a^j\right)\right) & a < 0 \end{cases} \quad (1)$$

where E_e is the instantaneous fuel consumption or emission rate of a pollutant species e; e can be CO, HC, and NOx; v and a represent the instantaneous vehicle speed (kilometers per hour), and acceleration (kilometers per hour per second) separately; $L_{i,j}^{e}$ and $M_{i,j}^{e}$ are the regression coefficients. A logarithm transform is adopted to avoid negative output and to enhance the model representativeness in low-speed and/or low-acceleration regimes. The model was created for positive and negative accelerations separately to ensure a better compliance with the measurement data over the full range of the vehicle-operation envelope.

1.3 Integrated Simulation Model

The requirements of developing environmentally sensitive traffic planning and management strategies have stimulated research efforts to integrate traffic, emission, and dispersion models. As traffic simulation models are commonly grouped into microscopic, mesoscopic, and macroscopic classes, they can be combined with corresponding emission models for estimation of traffic-induced air pollution at various scales. Because they describe detailed traffic activities, microscopic traffic models are widely used to compute dynamic emission quantities of road traffic with microscale emission models at a local network [8, 9]. However, since microscopic traffic and emission models are often computationally expensive, the performance of such integrated simulation may suffer from the lack of computing power because of the increased size of road networks in real applications.

Table 1 Vehicle classifications for two different types of emission models

ARTEMIS	VT-Micro
Petro Euro I	LDV1: Y<1990
Petro Euro II	LDV2: 1990≤Y<1995, E<3.2 l, M<83653
Petro Euro III	LDV3: Y ≥ 1995, E < 3.2 l, M < 83653
Petro Euro IV	LDV4: Y ≥ 1990, E < 3.2 l, M ≥ 83653
	LDV5: Y ≥ 1990, E ≥ 3.2 l
Diesel Euro I	LDT1: Y ≥ 1993
Diesel Euro II	LDT2: Y < 1993
Diesel Euro III	LDT high emitters

Y model year, *E* engine size, *M* mileage

In an early study [10], we described a computing platform capable of simulating, visualizing, and analyzing air quality impacts of traffic flow by integrating emission computation with microscopic traffic simulators. Besides the common off-line emission simulation approach, the system can run in an online mode, that is, it operates as a distributed computation server capable of simulating emission and dispersion of several road networks by real-time communication with clients running traffic simulations. At the present, an in-house traffic simulator, KTH-TPMA, and a commercial simulator, VISSIM, are integrated with the emission computing server based on the CORBA and Web Service technology. Figure 1 illustrates the data flow from traffic simulation to emission estimation procedures. The emission computation are triggered whenever there is a request from remote traffic simulation client. The emission estimation processes at the server side applies emission and air quality models to assess traffic impacts using received traffic activity information at different resolutions. With concerns on high-performance computing and flexibility, the system is fully distributed, which indicates potential to be coupled with different traffic models as well as system scalability, reliability, and efficiency. Figure 2 shows the graphical user interface of the emission estimation platform. The first graph shows the main window with the connected traffic clients and corresponding visualization of traffic states. The dynamic emission of the selected network area is presented in a time series chart in the second graph. The third graph demonstrates a visualization of the air quality map near the road network.

Several emission models have been implemented in the system for predicting traffic emissions and analyzing air quality. On the aggregate scale, both the MOBILE and ARTEMIS modules have been included for evaluation of general or average emission level. At the microscale, we have implemented models such as VT-Micro and VSP [11] with parameters proposed in the literature. Of course, functionality is provided for reconfiguration of the essential parameters of the models.

1.4 Objective

In order to apply the platform for dynamic estimation of traffic-induced emission and improve local traffic control measures in Stockholm, one key question is how to finely calibrate the adopted microscopic emission model. Usually, such calibration is based on the data collected using the chassis dynamometer or PEMS [12]. However, chassis dynamometers and PEMS systems are expensive, and a wide spectrum of vehicles needs to be measured to estimate a comprehensive model. Therefore, the experiment and later

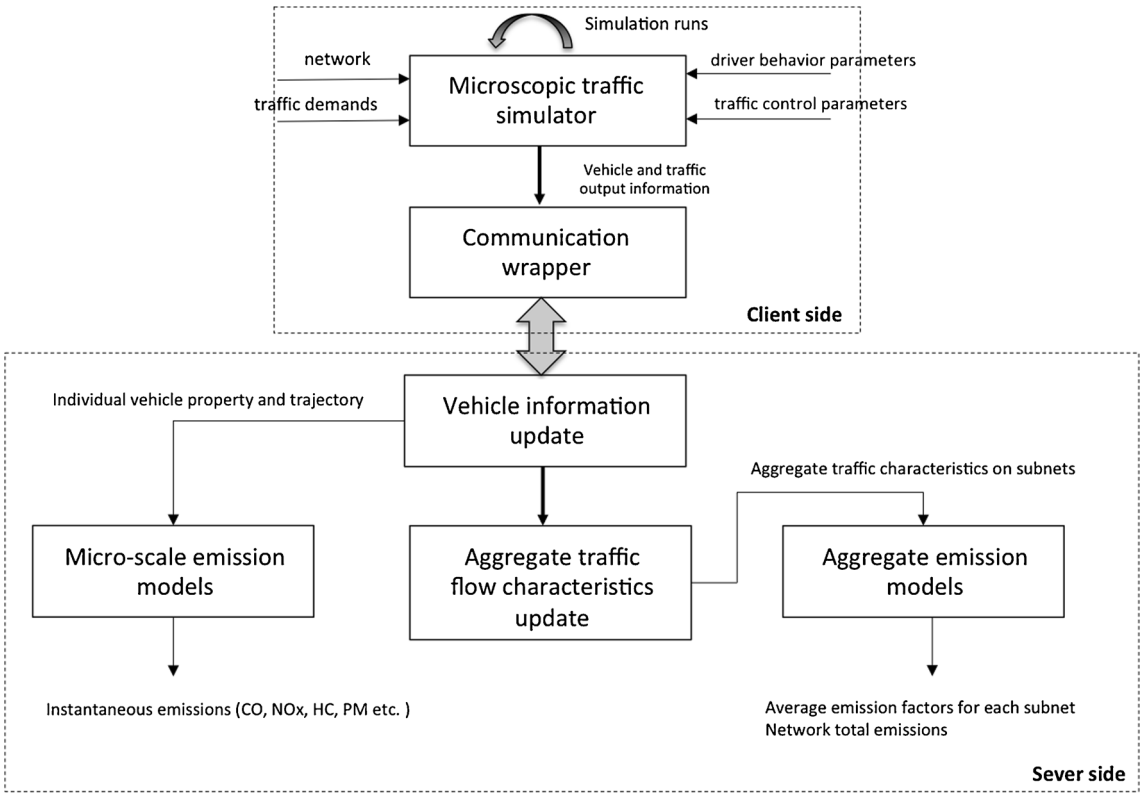

Fig. 1 Data flow of the traffic and emission modeling processes in the simulation platform

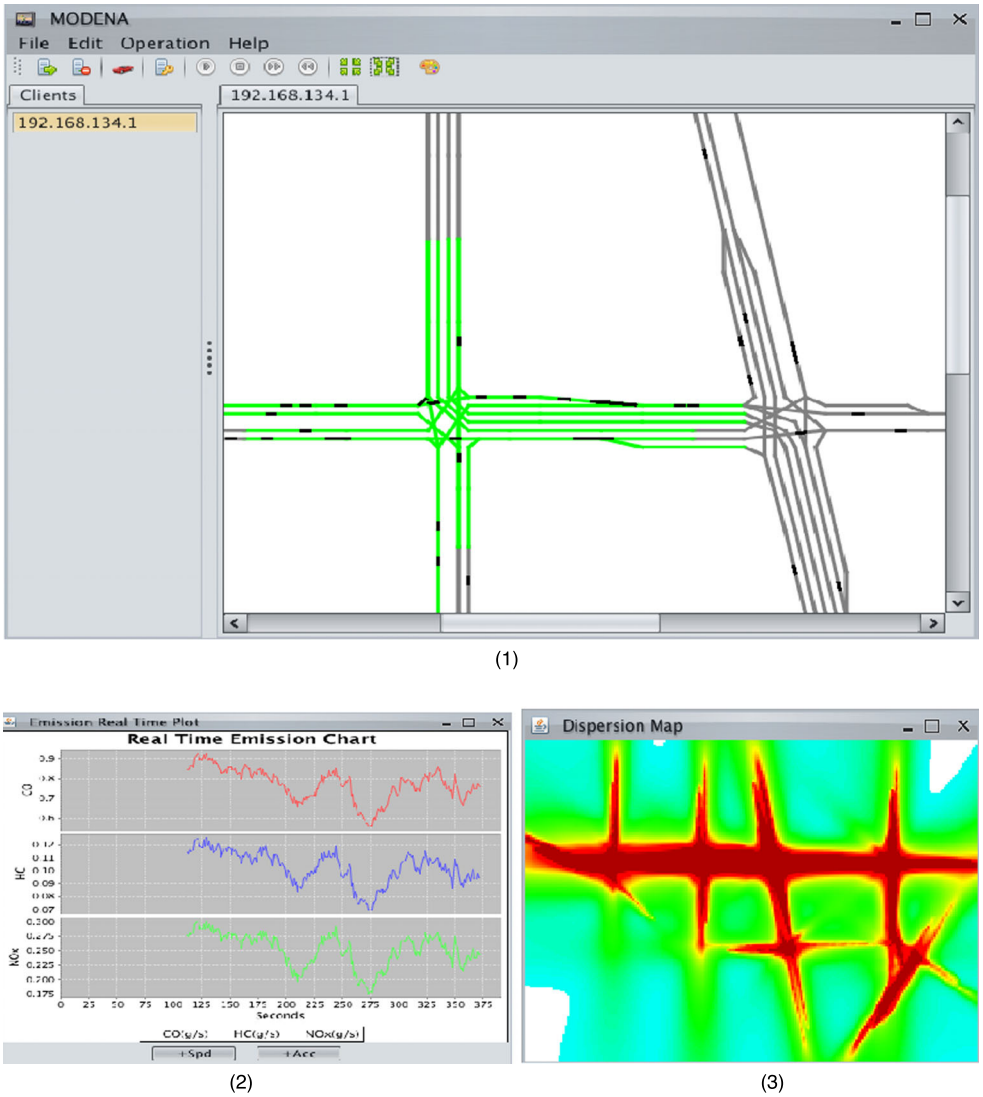

Fig. 2 The graphic user interface of the emission computing platform

data analysis are rather complicated and costly, especially for heavy-duty vehicles and buses. This paper demonstrates our recent research effort on developing a tuning approach for microscopic emission models given that dynamic emission measurement is not fully available. The basic idea is to calibrate microscopic emission models using aggregate emission information. The emission outputs of the EU ARTEMIS model are used as standard references due to its importance in the application projects supported by the Swedish Transport Administration.

2 Methodology

2.1 Problem Formulation

Similar to traffic models, microscale emission models need to be calibrated using real data before application. Whereas microscopic traffic models can be calibrated by different types of data, e.g., individual driver behavior or traffic flow measurement, microscopic emission models are conventionally estimated by instantaneous emission time series data at the individual vehicle level. However, such data is seldom available due to the large amount of expenses and work in data collection and analysis. Nevertheless, international collaboration is promoted on developing models of aggregate or average emission on roads [4] based on a wide spectrum of vehicle emission measurement. It is believed that vehicle emission can be estimated accurately at the aggregated level, given the differences among various vehicle types and individuals.

For calibration of microscopic impact models in this study, few instantaneous emission data is directly available. Therefore, the basic idea is, instead of using vehicle emission measurement data, to identify microscale emission models (mainly a regression emissions model, VT-Micro)

using aggregate emission information and instantaneous vehicle states generated by traffic simulation. Analytically, the calibration approach is formulated as a parameter identification problem according to aggregate emission measure estimated at a rougher resolution level on time and space. This is mathematically illustrated by the following:

$$\min_{\boldsymbol{\theta}} L(\boldsymbol{\theta}) = \int \int f(M(x,t,\boldsymbol{\theta}), A(x,t))\, dx\, dt \tag{2}$$

where $M(x,t,\boldsymbol{\theta})$ is the sum of the instantaneous emission of individual vehicles (estimated by microscale models) emitted at time t in subnet x; $A(x,t)$ is the aggregate emission estimated on the corresponding time and network; $\boldsymbol{\theta}$ is the parameter vector of the microscopic emission model; f is a statistical measure of the difference between the aggregated estimates M from the microscopic models and the aggregate estimates A from the aggregated model (e.g., ARTEMIS).

Although such formulation is not uncommon, the optimization solution method may suffer from the difficulties resulted from the under-determined nature of the nonlinear systems. In addition, the formulation of Eq. 2 misses an important factor. Although data used for estimating the original regression emission models (e.g., VT-Micro using data collected in the USA) reflects a different vehicle running condition from the Swedish case, the estimated parameters may reflect a latent structure of instantaneous vehicular emissions. Such information can be useful if it is incorporated in our model identification methodology. Therefore, we reformulate an objective function by taking into account of the difference of the estimated model parameters from their counterparts derived from real instantaneous vehicle emission data, i.e.

$$\min_{\boldsymbol{\theta}} O(\boldsymbol{\theta}, \lambda) = L(\boldsymbol{\theta}) + \lambda \cdot P(\boldsymbol{\theta}) \tag{3}$$

$$\text{where } P(\boldsymbol{\theta}) = \sum_{i=1}^{n} \left(\frac{\theta_i - \hat{\theta}_i}{\hat{\theta}_i} \right)^2$$

where $O(\boldsymbol{\theta}, \lambda)$ is the new objective function, and $P(\boldsymbol{\theta})$ is the penalty function representing the difference of the calibrated parameters from those estimated from measurement data elsewhere; λ is a non-negative penalty weight, which has a significant impact on the optimization result; θ_i and $\hat{\theta}_i$ are the ith element of the calibrated parameter vector $\boldsymbol{\theta}$ and the reference vector $\hat{\boldsymbol{\theta}}$ estimated by real data, respectively. When the statistical measure of scaled least square (LS) is applied, the Eq. 2 can be further represented in a discrete form as follows:

$$L(\boldsymbol{\theta}) = \sum_{k=1}^{K} \sum_{s=1}^{S} \left(\frac{M(s,k,\boldsymbol{\theta}) - A(s,k)}{A(s,k)} \right)^2 \tag{4}$$

where s and k are discrete representation of space and time.

Comparing the microscopic VT-Micro models and aggregate ARTEMIS model, their vehicle classifications are not fully compatible. Whereas VT-Micro classifies vehicles based on the vehicle information, such as model year, engine size, and mileage, ARTEMIS groups vehicles according to the fuel type and emission standards such as Euro I–IV. Since the aggregate estimation of ARTEMIS is used as the reference, the parameters of the VT-Micro model will be estimated according to the ARTEMIS vehicle-type classification.

2.2 Model Estimation Approach

To solve the parameter identification problem formulated in Eq. 3, it is widely accepted to resort to numerical optimization methods. The objective function of Eq. 4 involves calculation of aggregated emissions A as well as computation of dynamic emissions M using simulated traffic data. Microscale emissions M are calculated from traffic simulation data and the parameters $\boldsymbol{\theta}$ of the emissions regression model. The aggregate emissions A are calculated by ARTEMIS using aggregate traffic characteristics derived from the simulated data.

A numerical optimization technique is used to find the parameters $\boldsymbol{\theta}$ that solve Eq. 3. The iterative optimization process starts with an initial guess on the parameter vector $\boldsymbol{\theta}_0$. For each iteration k, the emission of the ARTEMIS and microscale model will be estimated using the parameter vector $\boldsymbol{\theta}_k$ and simulated traffic states. Then these emission outputs and the parameter vector $\boldsymbol{\theta}_k$ will be used to compute the objective function $O(\boldsymbol{\theta}_k, \lambda)$. If the selected convergence condition is fulfilled, $\boldsymbol{\theta}_k$ will then be the final optimal solution and the numerical search terminates; otherwise, the optimization process continues to the next iteration by repeating the computational steps.

Among many nonlinear optimization algorithms, the simultaneous perturbation stochastic approximation approach (SPSA) [13] is a numerical scheme using first-order approximation of the gradient vector of the optimization objective function. It shows apparent advantages over the conventional finite difference scheme (FDM). It is computationally more efficient especially for high-dimension multivariate optimization problems because only two evaluations of the objective function per iteration are necessary in SPSA. On the other hand, the FDM algorithm needs $2n$ evaluations (n is the dimension of the parameter vector). In addition, the SPSA achieves the same level of accuracy as the FDM algorithm if the same number of iterations are performed.

The SPSA algorithm can be mathematically expressed as follows:

$$a_k = \frac{a}{(k+A)^{\alpha}} \tag{5}$$

$$c_k = \frac{c}{k^{\gamma}} \tag{6}$$

$$\boldsymbol{\theta}_k^{+} = \boldsymbol{\theta}_k + c_k \cdot \Delta \tag{7}$$

$$\boldsymbol{\theta}_k^{-} = \boldsymbol{\theta}_k - c_k \cdot \Delta \tag{8}$$

$$\hat{g}_k = \frac{O(\boldsymbol{\theta}_k^{+}, \lambda) - O(\boldsymbol{\theta}_k^{-}, \lambda)}{2 \cdot c_k \cdot \Delta} \tag{9}$$

$$\boldsymbol{\theta}_{k+1} = \boldsymbol{\theta}_k - a_k \cdot \hat{g}_k \tag{10}$$

where a_k and c_k are gain sequences at step k; Δ is a n-dimensional random perturbation vector drawn from a Bernoulli distribution; $\hat{g}_k$ is the estimated gradient vector at step k; a, A, α, γ, and c are user-defined parameters for the algorithm. The literature [13, 14] suggests that

- α, γ can be set as 0.602 and 0.101, respectively, the asymptotically optimal values of 1.0 and 1/6 may also be used.
- A is chosen such that it is much less than the maximum number of iterations allowed or expected, normally, taking 10 % of maximum iteration number.
- Choose a such that a/A^{γ} times the magnitude of elements in $\hat{g}_0$ approaches smallest desired change in the first few iterations of $\boldsymbol{\theta}$, which requires some extra replications in early iterations.

2.3 Enhancements on SPSA

Although the basic SPSA algorithm has proved to be powerful in solving optimization problems, enhancement on the algorithm is still necessary to make it more suitable for numerical analysis in this study.

2.3.1 Scaling

In the dynamic emission model, model parameters may have significantly different orders of magnitude. For example, in the estimation of the VT-Micro model [7], the largest absolute coefficient value is 8.27978, and the smallest is 3.98×10^{-8}. In practice, this will cause numerical difficulties in the optimization. Scaling can dramatically improve the performance of the SPSA algorithm [15, 16]. In this study, a simple scaling is implemented for each parameter to transfer them into a value between 1 and 10. When applying parameters for emission computation in SPSA, an inverse scaling has to be performed.

2.3.2 Gradient Average

In principle, averaging a few gradient estimations can improve the precision of the estimate of gradient information [17]. This is also emphasized by [18]. Thus, in our implementation, we consider incorporating several independent SPSA gradient approximations at each iteration. That is, we replace the original calculation of $\hat{g}_k$ in Eq. 9 by the following:

$$\hat{g}_k = \frac{1}{r} \cdot \sum_{j=1}^{r} \hat{g}_k^{(j)} \tag{11}$$

where r is the replication number of independent SPSA approximations. According to the report in [14], the averaged gradients mechanism does not give significant performance improvement in comparison with using standard SPSA algorithm when the sample size is small. Along with the increase of the sample size, the advantage of gradient average becomes obvious. Even though a larger size of replications may produce better performance, the computation needs extra calculations on gradients per iteration. When the evaluation of the objective function is expensive, the computational cost on replications will increase dramatically. Thus, a trade-off has to be made between optimization speed and quality. In the implementation, r is normally set to 4 which gives empirically satisfactory results.

2.3.3 Multiple Initial Guesses

Although the SPSA approach has shown to be powerful in the literature, it still belongs to a gradient search algorithm. It is widely known that gradient-based approaches may suffer from the existence of local optima. In this problem, we consider a classical mechanism by introducing multiple random initial guesses. Therefore, the smallest optimum will be our final solution after running the SPSA algorithm from each initial guess.

3 Numerical Experiments and Results

Numerical experiments are conducted for each vehicle class and each emission factor using the following steps:

- Generate microscopic vehicle states by a traffic simulator and determine the model calibration and validation datasets;
- Test and choose constant parameters for the numerical scheme including the SPSA algorithm coefficients and termination condition;
- Test and analyze the effect of the penalty weight λ by solving the optimization problem using a small amount

of simulated data and select an appropriate λ for the calibration process;
- Solve the numerical optimization problem using the whole calibration dataset;
- Perform model validation using validation datasets.

3.1 Experiment Preparation

3.1.1 Traffic Simulation Network

In our studies, dynamic traffic states are generated by microscopic traffic simulators, mainly the KTH-TPMA and VISSIM. This paper is focused on the results using KTH-TPMA, a traffic simulation model developed at our university. Two road networks are used for calibration and validation studies, including a big intersection and a relatively large road network in a Swedish city. The geometrical configuration of the networks are depicted in Fig. 3. In order to use simulated traffic data to represent stochastic traffic conditions and fit the models with confidence, replications have to be carried out with an independent random seed for each simulation run [19]. This numerical study uses 20 simulation replications to generate representative datasets. For the first network, a 1-h traffic data is generated by simulation for calibration and validation using different random seeds. Twenty-minute traffic data generated on the second road network is mainly used for validation. Before collecting data from the traffic model, the simulator had been running for 15 min to avoid the vehicle loading effect in the beginning of a simulation.

3.1.2 Selection of the SPSA Coefficients

According to initial tests, the performance of SPSA is quite sensitive to the coefficients in numerical optimization. With careful numerical experiments according to the guidance of the previous section, the coefficients listed in Table 2 are adopted, and M_d is the least desired change magnitude in the early iterations. c is chosen to be 0.01 in order to prevent the gradient $g_k(\boldsymbol{\theta}_k)$ from being too large in its magnitude, and a is selected so that the risk of divergence is reduced in early iterations, whereas the performance in the later iterations is enhanced especially when the step size is small.

3.1.3 Global Solution

For a certain penalty weight λ, the optimization problem is solved by sampling N random initial points and then running the SPSA algorithm from each of these points. The final parameter vector leading to the smallest objective function will be considered as the global solution to the optimization problem with the λ value. Although the increase of the initial guesses may raise the chance of finding a global solution, the computational time will also grow dramatically. In the study, $N = 100$ to 1000 is used to realize a trade-off between the chance for a global solution and computational time.

3.2 Calibration Study

3.2.1 Termination Condition

For SPSA, two types of termination conditions could be used in numerical experiment for justification of convergence:

- $|\boldsymbol{\theta}_k - \boldsymbol{\theta}_{k-1}| \leq \epsilon_x$
- $|O(\boldsymbol{\theta}_k, \lambda) - O(\boldsymbol{\theta}_{k-1}, \lambda)| \leq \epsilon_y$

where ϵ_x and ϵ_y are small positive values to determine the termination of the optimization process. Although the first condition gives more reliable performance especially when

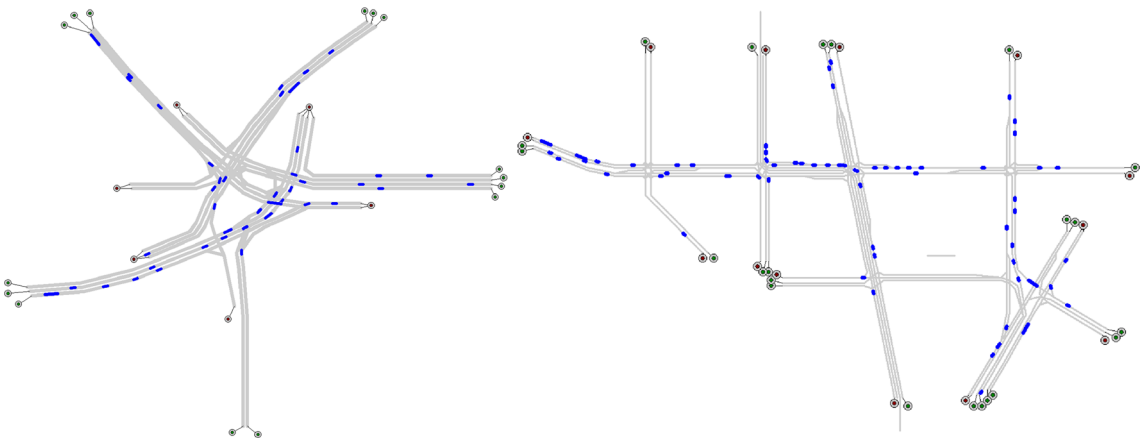

Fig. 3 Configuration of the road networks used for calibration and validation in numerical experiment (*left* is net1 and *right* is net2)

Table 2 The SPSA coefficients used in the application

Variable	Literature	Application
a	$\frac{a}{A^\gamma} \cdot \lvert\hat{g}_0\rvert \approx M_d$	$\frac{a}{A^\gamma} \cdot \lvert\hat{g}_0\rvert \approx 0.1$
A	10 % iteration	100
c	Related to std. dev. of noise in $O(\boldsymbol{\theta}, \lambda)$	0.01
α	1.0 or 0.602	0.602
γ	1/6 or 0.101	0.101

random noise is involved in the objective function, both conditions can be applied for this optimization problem.

A series of numerical experiments are conducted to evaluate the configuration of ϵ_x and ϵ_y for different λ values and various vehicle classes and emission types. Figure 4 illustrates examples of numerical convergence when the CO emission model for the Petro Euro II vehicle class is calibrated ($\lambda = 10^{-5}$). It can be concluded that convergence is fulfilled when the termination conditions of $\epsilon_x = 10^{-6}$ and $\epsilon_x = 10^{-7}$ are applied. However, the process stops too early when $\epsilon_x = 10^{-5}$ is adopted. Meanwhile, when ϵ_x is set to be 10^{-7}, many iterations of computation are wasted. Similar phenomenon happens when the convergence condition on the objective function is applied. In our analysis, the convergence condition on the adaption of the parameter vector is used, and the configuration of ϵ_x needs careful tests. For example, $\epsilon_x = 10^{-6}$ is adopted in the illustrated example.

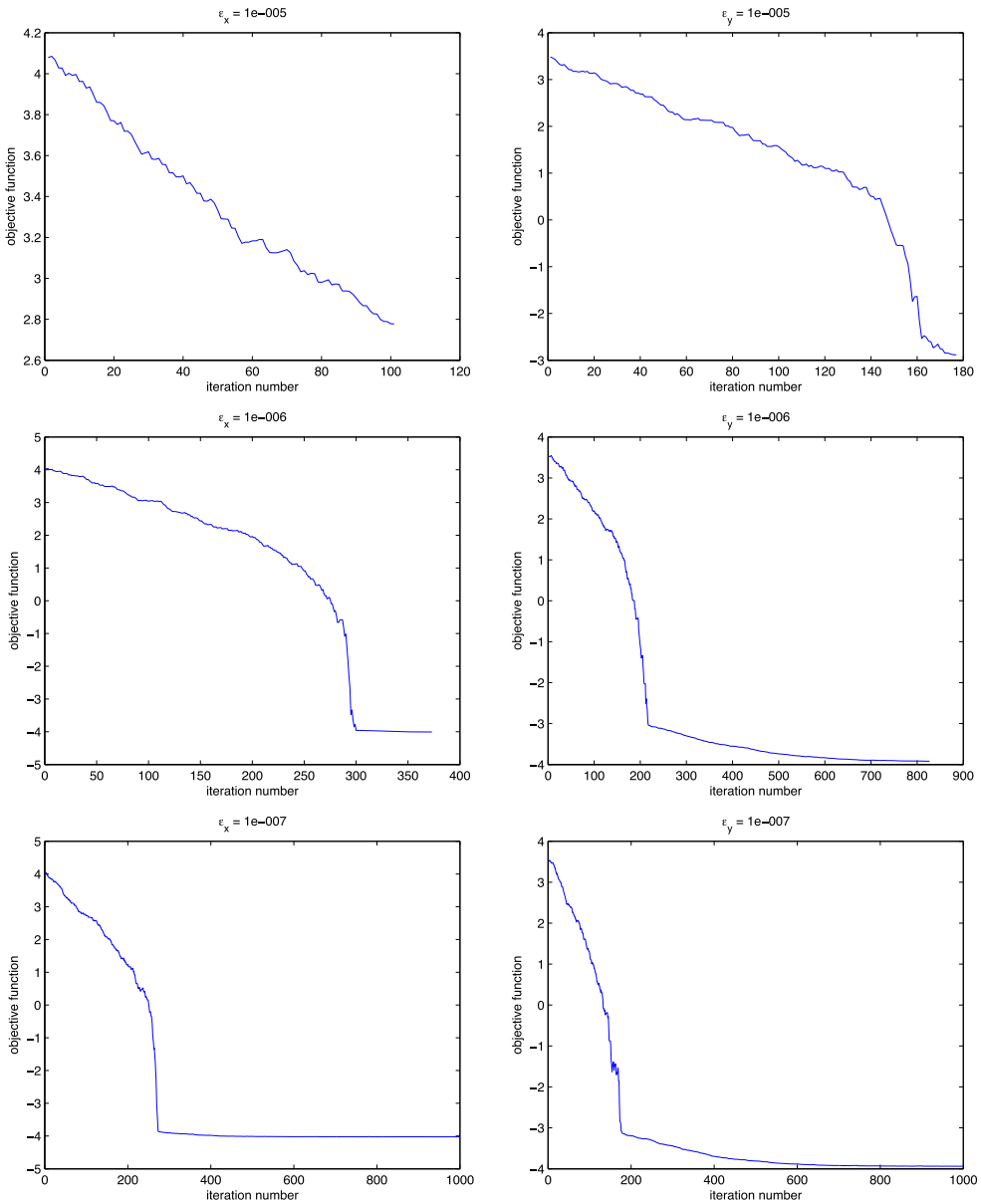

Fig. 4 Comparison of the convergence performance of the objective function (in logarithm) defined by Eq. 3 when different termination conditions are applied

3.2.2 Influence of λ

It is important to analyze the effect of penalty weight on the final result of the optimization problem. In principle, the influence of λ for the optimization is quite obvious:

- when λ approaches zero, the optimal solution tends to minimize $L(\boldsymbol{\theta})$;
- when λ approaches infinity, the optimal solution tends to minimize the penalty term $\lambda \cdot P(\boldsymbol{\theta})$.

A proper λ value is expected to balance the roles of $L(\boldsymbol{\theta})$ and $P(\boldsymbol{\theta})$, that is, ensuring the two parts having appropriate influences on the general objective function. While it is difficult to directly analyze the relation between λ and $O(\boldsymbol{\theta}, \lambda)$ or $L(\boldsymbol{\theta})$, the proportion of $L(\boldsymbol{\theta})$ in the total objective function $O(\boldsymbol{\theta}, \lambda)$ (i.e. $L(\boldsymbol{\theta})/O(\boldsymbol{\theta}, \lambda)$) is introduced as an intermediate variable to study the relations between λ and other functions ($O(\boldsymbol{\theta}, \lambda)$, $\lambda P(\boldsymbol{\theta})$, and $L(\boldsymbol{\theta})$). It is found that with the increase of penalty weight λ both $O(\boldsymbol{\theta}, \lambda)$ and $\lambda \cdot P(\boldsymbol{\theta})$ raise up. But the impact of λ on $L(\boldsymbol{\theta})$ is difficult to conclude.

In the calibration, it is also important to find an appropriate range of λ values so that the effect of penalty weight can be better understood. The final determination of the proper λ value is mainly based on the empirical cross-validation result. For instance, during the calibration of the CO emission model for the Petro Euro II vehicle class, a sensitivity range of $[10^{-6}, 10^{-4}]$ is found, which means $\lambda < 10^{-6}$ or $\lambda > 10^{-4}$ does not give solution significantly different from $\lambda = 10^{-6}$ or $\lambda = 10^{-4}$, respectively. Therefore, λ values in a grid defined between 10^{-6} and 10^{-4} (with an interval of 10^{-6}) are applied for model calibration. Cross-validation is performed on the calibrated parameters with different λ values. Examples of validation results are shown in Fig. 5 when different λ values, such as 10^{-4}, 5×10^{-5}, 2×10^{-5}, and 10^{-5}, are applied for optimization. The validation is conducted using simulated traffic data of one hour on the first network (net1).

It is clear that the model performance is worst when the weight λ is too large. This indicates that the emphasis on the reference parameter vector may result in the difficulty of minimizing $L(\boldsymbol{\theta})$. On the other hand, small penalty term, e.g. $\lambda = 10^{-5}$, may lead to the emphasis on $L(\boldsymbol{\theta})$, therefore increasing potential over-fitting risk. In the example, a good result on fitness is achieved when $\lambda = 2 \times 10^{-5}$ is applied.

3.2.3 Final Parameters

This study applies the reference parameters of the VT-Micro regression model estimated based on on-road PEMS measurements of 30 petrol passenger cars including two Euro

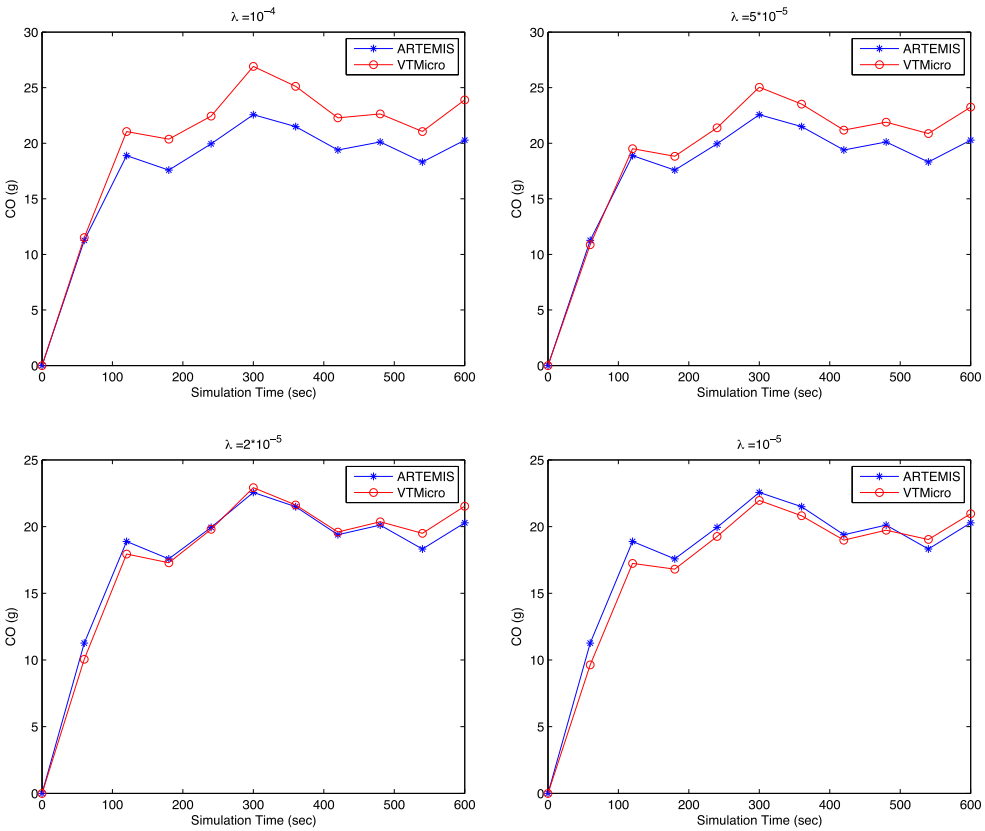

Fig. 5 Comparison of the validation results for different λ settings

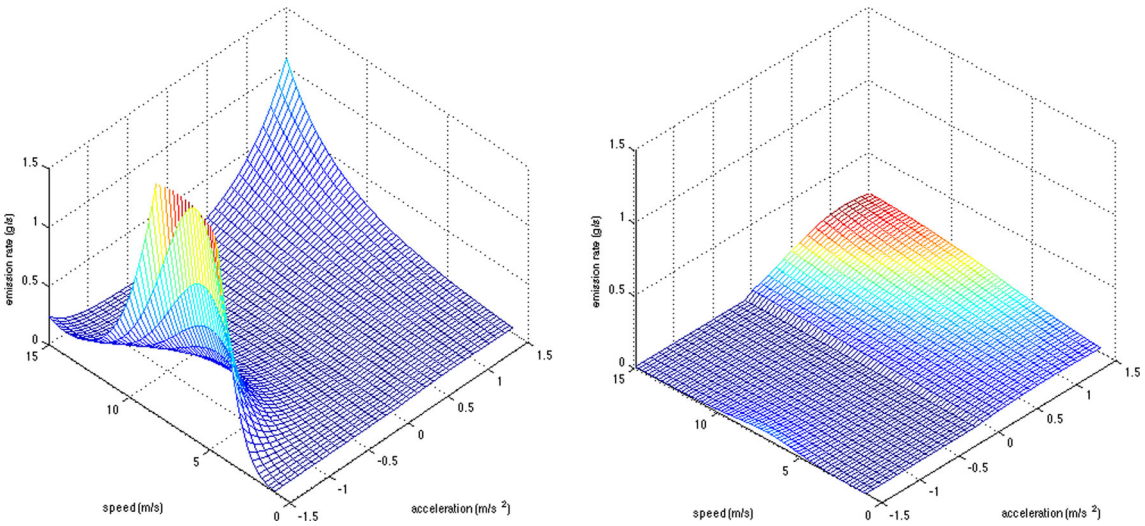

Fig. 6 Comparison of the calibrated microscopic model (*right*) on the CO emission with the reference model (*left*)

I vehicles, fifteen Euro II vehicles, twelve Euro III vehicles and one Euro IV vehicle [12]. Although the European emission standard is applied for cars in the experiment, they are not operating in the same conditions as the European vehicles.

The model calibration is based on 1-h traffic data simulated using "net1," the first road network of Fig. 3 (not including the vehicle loading time at the beginning of each simulation). Figure 6 compares the CO emission maps of the Petro Euro II category predicted by the emission models using the reference and calibrated parameters, respectively. It is not difficult to observe that the CO emission outputs of the two models are in different magnitudes. The calibration process results in the adaption of the CO emission output at a lower level whereas the characteristics of the model are to some degree kept. For instance, accelerations at high speeds lead to more CO emissions and this phenomenon becomes more obvious in the emission map predicted by the calibrated model.

3.3 Validation

To evaluate the performance of the calibrated model, the prediction of the estimated VT-Micro model is aggregated and then compared with the estimation of ARTEMIS using the simulated traffic data on two different networks. A widely used statistical measure, mean absolute percentage error (MAPE), is adopted to analyze the performance. The calculation of MAPE can be expressed by

$$\text{MAPE} = \frac{1}{m}\sum_{i=1}^{m}\left|\frac{M_i - A_i}{A_i}\right| \tag{12}$$

where M_i and A_i are accumulated emission of VT-Micro and the estimation of ARTEMIS in time interval i, respectively, and m is the total number of intervals.

Table 3 summarizes the general validation results for three datasets (net1-10, net1-60, and net2-20). The net1-10 and net-60 datasets include 10-min and 1-h simulated traffic data of "net1," respectively. The net2-20 dataset is 20-min simulated data of the second network "net2." It can be concluded that the calibrated model shows generally good prediction performance in comparison to the aggregate estimation of ARTEMIS. For CO, the largest errors (about 35 %) occur in the vehicle categories of Euro I and Euro IV, in which insufficient data was collected (from two Euro I and one Euro IV vehicles) for the estimation of the reference parameters. The worst performance mainly happens for the validation using traffic data simulated from

Table 3 Validation results in terms of MAPE (percentage) for different emission factors using three datasets

Emissions	Petro Euro I			Petro Euro II			Petro Euro III			Petro Euro IV		
	net1-10	net1-60	net2-20	net1-10	net1-60	net2-20	net1-10	net1-60	net2-20	net1-10	net1-60	net2-20
CO	3.45	5.27	34.92	12.76	3.94	6.46	3.61	3.63	13.11	7.60	8.94	35.92
HC	1.95	3.78	7.87	0.82	0.55	5.78	2.00	3.78	12.08	3.61	6.39	10.85
NOx	7.31	3.52	11.82	4.84	3.87	2.97	2.06	2.82	10.16	3.54	5.59	25.09

the second network, which is independent from the calibration dataset. The validation on HC shows better results than CO according to the MAPE measures. The relatively worse performance also happens to the cross-validation case using data from the second network. For NOx, the validation results are satisfying except that the cross-validation error for the Euro IV type reaches 25 %. For all three types of emissions, the relatively poorer performance on cross-validation indicates that traffic pattern may play important roles to the results of model identification. Especially, the first network is a large intersection with mainly stop-and-go traffic, whereas the second network describes traffic in a much bigger area of six intersections. Random vehicle driving cycles from the two networks show different statistical property.

4 Conclusions

This paper starts with an illustration on integrated traffic and emission modeling and their increasing importance in project-level traffic management applications. It then raises the dynamic emission model tuning issue for accurate local traffic impact assessment. Inspired by the calibration approaches for microscopic traffic models using aggregate traffic flow data, the study proposes a numerical approach to calibrate microscopic emission model using aggregate emission estimation. This indicates that different aggregate data sources can be applied, not only average vehicle emission but also air quality information, considered as a function (dispersion process) of aggregate traffic emission in reality.

Numerical experiments are conducted in a case study, through which VT-Micro, a microscopic regression-based emission model, is finely tuned by aggregate emission levels estimated by ARTEMIS, a widely accepted EU aggregate emission estimator. Based on the ARTEMIS estimation and reference parameters derived from some limited PEMS data, the microscale VT-Micro model is calibrated for each ARTEMIS vehicle class while minimizing an objective function combining:

- a scaled measure on the aggregate output difference between VT-Micro and ARTEMIS models; and
- a scaled measure on the Euclidean distance between the calibrated and reference parameter vectors.

The standard SPSA algorithm with several critical enhancements is applied to solve the multivariate optimization problem. Extensive numerical experiment has been conducted to analyze the effects of the SPSA coefficients, penalty weight, size of road segments, etc. The calibrated parameter vectors are validated by the following:

- traffic data generated at the same road network but with different random seeds;
- traffic data simulated from another road network with different traffic flow characteristics.

According to the validation results, the calibration approach shows its capacity in identifying dynamic emission model parameters especially when only aggregate emission information is available. The estimated models are implemented in an integrated traffic and emission simulation platform potentially applicable for project-level traffic environment analysis. While the second-by-second traffic states were generated using an in-house traffic simulation tool in this study, promising results are also achieved when traffic data generated by a commercial microscopic traffic simulator, VISSIM, is used for emission model calibration and validation. However, a limitation of this study is the assumption that the model outputs from ARTEMIS for different aggregate time intervals are reliable emission estimates. With the increasing availability of roadside emission measurement, the method has a large potential to be further extended in the new arena.

Acknowledgments The authors would like to express their gratitude to the Swedish Transport Administration (MEMFIS project) and J. Gustav. Richert Stiftelse (MOPED project) for their support on the emission modeling study. The study on integrated traffic and emission simulation was funded by the Swedish National Energy Agency through the Basic Energy Research programme of the Swedish Research Council.

References

1. EPA (2002). *Users guide to MOBILE 6.0: mobile source emission factor model. Technical report EPA420-R-02-001*. Washington: Environmental Protection Agency.
2. Ntziachristos, L., & Samaras, Z. (2000). *Copert III: computer programme to calculate emissions from road transport. Technical report 49*. Copenhagen: European Environment Agency.
3. Hausberger, S., Rexeis, M., Zallinger, M., Luz, R. (2009). *Emission factors from the model PHEM for the HBEFA version 3. Technical report, Institute for Internal Combustion Engines and Thermodynamics*. Graz University of Technology.
4. Keller, M., & Kljun, N. (2007). *ARTEMIS road emission model—model description*. Zurich: INFRAS.
5. Sjödin, A., & Jerksjö, M. (2008). Evaluation of European road transport emission models against on-road emission data as measured by optical remote sensing. In: *17th International transport and air pollution conference*.
6. Barth, M., An, F., Younglove, T., Scora, G., Levine, C., Ross, M., Wenzel, T. (2000). *Development of a comprehensive modal emissions model. Final report project 25–11*. Washington: National Cooperative Highway Research Program.
7. Rakha, H., Ahn, K., Trani, A. (2004). Development of VT-Micro model for estimating hot-stabilized light duty vehicle and truck emissions. *Transportation Research Part D*, *9*, 49–74.

8. Stathopoulos, F., & Noland, R. (2003). Induced travel and emissions from traffic flow improvement projects. *Transportation Research Record, Journal of TRB*, *1842*, 57–63.
9. Stevanovic, A., Stevanovic, J., Zhang, K., Batterman, S. (2009). Optimizing traffic control to reduce fuel consumption and vehicular emissions. *Transportation Research Record: Journal of the Transportation Research Board*, *2128*, 105–113.
10. Huang, Z., & Ma, X. (2009). Integration of emission and fuel consumption computing with traffic simulation using a distributed framework. In: *Proceedings of 12th international IEEE conference on intelligent transportation system*.
11. Frey, H.C., Unal, A., Chen, J., Li, S. (2003). Modeling mobile source emissions based upon in-use and second-by-second data: development of conceptual approaches for EPA's new moves model. In: *Proceedings of the annual meeting of the air and waste management association*, Pittsburgh.
12. Ma, X., Lei, W., Andréasson, I., Chen, H. (2012). An evaluation of microscopic emission models for traffic pollution simulation using on-board measurement. *Environmental Modeling & Assessment*, *17*(4), 375–387.
13. Spall, J. (1998). Implementation of the simultaneous perturbation algorithm for stochastic optimization. *IEEE Transactions on Aerospace and Electronic Systems*, *34*(3).
14. Pflug, G. (1996). *Optimization of stochastic models: the interface between simulation and optimization*. New York: Springer.
15. Hill, S., Gerencsér, L., Vágó, Z. (2003). Stochastic approximation on discrete sets using simultaneous perturbation difference approximations. In: *Proceedings on information science and systems*.
16. Garrett, J. (2004). Jointly optimizing model complexity and data-processing parameters with mixed-inputs. In: *Computing science and statistics proceedings of the symposium on the interface*.
17. Kocsis, L., & Szepesvári, C. (2006). Universal parameter optimisation in games based on SPSA. *Machine Learning*, *63*, 249–286.
18. Spall, J. (1992). Multivariate stochastic approximation using a simultaneous perturbation gradient approximation. *IEEE Transaction on Automatic control*, *37*, 332–341.
19. Law, A.M., & Kelton, W.D. (2000). *Simulation modeling and analysis*, 3rd edn. New York: McGraw-Hill Higher Education.